

DOI: 10.13208/j.electrochem.131129

Artical ID:1006-3471(2014)05-0470-06

Cite this: *J. Electrochem.* 2014, 20(5): 470-475

Http://electrochem.xmu.edu.cn

固体氧化物燃料电池 Cu-LSCM-CeO₂/LSCM-YSZ/Ni-ScSZ 复合阳极制备及性能

吕尧, 黄波*, 顾习之, 侯春一, 胡一星, 王晓颖, 朱新坚

(上海交通大学机械与动力工程学院燃料电池研究所, 上海 200240)

摘要: 采用流延法制得 LSCM-YSZ 阳极支撑层 /Ni-ScSZ 阳极活性层 /ScSZ 电解质层复合膜, 在 LSCM-YSZ 支撑层上印刷一层 Cu-LSCM-CeO₂ 阳极催化层, 即 Cu-LSCM-CeO₂/LSCM-YSZ/Ni-ScSZ 功能梯度层阳极. 研究表明, Cu/LSCM/CeO₂ 质量配比为 2:7:1 功能梯度阳极 (LSCM-YSZ2010) 有较好的性能, 单电池以氢气和乙醇为燃料 (750 °C) 最大功率密度分别为 511 和 390 mW·cm⁻². 单电池稳定性实验表明, LSCM-YSZ2010 阳极单电池以乙醇为燃料 750 °C 长时间运行 218 h, 性能稳定. X-射线能量散射分析表明该阳极具有较好的抗碳沉积性能.

关键词: 固体氧化物燃料电池; 催化层; 碳沉积; 阻抗谱; 电化学性能

中图分类号: TM911

文献标识码: A

固体氧化物燃料电池 (SOFC) 可以将储存在燃料中的化学能直接转化为电能, 具有能量转化效率高、环境友好、燃料适应性强的优点^[1-3]. 传统的 Ni/YSZ 金属陶瓷阳极当直接使用碳氢化合物燃料时, 发生碳沉积, 降低电池性能^[4-7], 因此适宜的碳氢化合物燃料阳极材料一直备受关注. Cu-CeO₂-YSZ 系^[8-12]、氧化铈系^[13-17]、钙钛矿结构氧化物^[18-22]等阳极材料已被深入地研究. 氧化铈的中温电子导电率和电催化活性均不佳, 需掺入 Ni 金属. Cu-CeO₂-YSZ 系中 Cu 对碳氢化合物燃料的裂解反应活性不高, 虽可抑制碳沉积, 但 Cu 及其化合物的熔点低, 难与 CeO₂ 烧结, 故多采用反复浸渍, 该法耗时耗能, 且质量控制困难. 钙钛矿结构的陶瓷基阳极 (如掺杂的 LaCrO₃ 和 SrTiO₃) 抗碳沉积性较优良, 而其活性差. 因而研究目标更多转移至新型阳极结构. Barnett 等^[23-24]将 Ru-CeO₂ 催化层置于传统的 Ni-YSZ 阳极, 取得了较好的效果. 而该催化层 Ru 价格昂贵及在一定温度下还会生成 RuO₄^[25]. Wang 等^[26]采用 Ru-Al₂O₃ 催化层代替 Ru-CeO₂ 催化层, 该催化层具有极佳的稳定性以及与 Ni-YSZ 良好的兼容性, 且碳沉积量极少, 但 Ru 价格昂贵难以推广. Hornés 等^[27]采用 Cu-Ni-CeO₂ 阳极材料, 对甲烷有强电催化分解作用, 但仍有少量的碳沉

积. Yun 等^[28]将 SDC 包覆于 Ni/SDC 阳极且取得了极佳的效果, 该阳极运行 180 h 后性能无明显衰减, 但碳沉积问题仍未改善. Zhu 等^[29]将 Ni-La_xCe_{1-x}O_y 催化层置于 Ni-SDC 阳极, 其电催化活性很好, 并在一定程度抑制了碳沉积. Jin 等^[30]将 Cu_{1.3}Mn_{1.7}O₄-SDC 催化层置于 Ni-SDC 阳极, 其电催化性能极佳, 然而催化层以及阳极仍有少量碳沉积.

钙钛矿结构 (ABO₃) 的陶瓷基阳极材料 (如掺杂的 LaCrO₃) 在碳氢化合物燃料中的电导率低, 但仍有一定的电催化活性, 能抗碳沉积, 且其氧化还原循环过程的体积变化很小. 本文采用复合流延共烧结和丝网印刷法制得 Cu-La_{0.75}Sr_{0.25}Cr_{0.5}Mn_{0.5}O₃ (LSCM)-CeO₂/LSCM-YSZ/Ni-ScSZ/ScSZ 复合膜, 采用功能梯度阳极相配方式, 以期降低碳氢化合物燃料发电时的碳沉积. 功能梯度阳极的 Cu-LSCM-CeO₂ 催化层, 实现碳氢化合物的阳极表面电催化氧化, 避免碳沉积; LSCM-YSZ 阳极支撑层, 支撑整个阳极复合膜; Ni-ScSZ 阳极活性层, 提高电催化活性. 以氢气和乙醇蒸汽为燃料, 氧气为氧化剂, 构筑以 Cu-LSCM-CeO₂/LSCM-YSZ/Ni-ScSZ/ScSZ 为阳极的 SOFC 单电池.

1 单电池与测试

阳极: 用乙醇和丁酮的共沸物作溶剂, 加入粉

料(ScSZ、NiO-ScSZ 及 LSCM-YSZ),粘结剂(PVB: 10%~15%),分散剂(三乙醇胺:1%~3%),增塑剂(聚乙二醇:6%~9%)和造孔剂(草酸氨:10%~15%)球磨 4 h 制浆,3 次流延制得 LSCM-YSZ 阳极支撑层/Ni-ScSZ 阳极活性层/ScSZ 电解质复合膜,于 1400 °C 烧结 3 h,即得复合膜($\phi=14\text{ mm}$).

阴极: $(\text{Pr}_{0.7}\text{Ca}_{0.3})_{0.9}\text{MnO}_3$ (PCM) 与松油醇按质量比 1:0.7 混合制浆,经丝网印刷沉积至电解质 ScSZ 上,1200 °C 烧结 2 h 即可,组合构成 Ni-ScSZ/ScSZ/PCM 单体电池. 低温燃烧法合成 $\text{La}_{0.75}\text{Sr}_{0.25}\text{Cr}_{0.5}\text{Mn}_{0.5}\text{O}_3$ ^[31] 和 Cu-CeO₂ 粉体^[32],将粉体与松油醇混合成浆料,经丝网印刷沉积到阳极支撑层 LSCM-YSZ 上,于 1150 °C 烧结 2 h 得 CuO-LSCM-CeO₂/LSCM-YSZ/Ni-ScSZ 功能梯度层阳极, 燃料电池阳极 H₂ 气氛中还原成 Cu-LSCM-CeO₂/LSCM-YSZ/Ni-ScSZ. Cu/LSCM/CeO₂ 按质量配比制备不同的催化层,其中,15%Cu-70%LSCM-15%CeO₂、20%Cu-70%LSCM-10%CeO₂、22.5%Cu-70%LSCM-7.5%CeO₂ 分别标示为 LSCM-YSZ1515、LSCM-YSZ2010 和 LSCM-YSZ3010.

单电池:将由阳极、催化层、电解质及阴极组成的单电池密封于 Al₂O₃ 管的一端,管内通氧气,管外通 H₂ 或者乙醇蒸汽. 采用电化学工作站 (PARSTAT4000, America) 测试单电池的 I - V 曲线以及交流阻抗谱图. 用扫描电子显微镜 (SEM, Sirion 200) 观察阳极形貌.

2 结果与讨论

图 1、2 给出 LSCM-YSZ1515、LSCM-YSZ2010

和 LSCM-YSZ3010 阳极单电池的氢气和乙醇燃料 (750 °C、800 °C) 的 I - V 曲线与 I - P 曲线. 从图可见, LSCM-YSZ2010 阳极单电池在 750 °C 最大功率密度分别为 511 mW·cm⁻² (氢气) 和 390 mW·cm⁻² (乙醇),而 LSCM-YSZ1515 阳极单电池,最大功率密度分别是 228 mW·cm⁻² (氢气) 和 165 mW·cm⁻² (乙醇). 在 800 °C 下, LSCM-YSZ1515 为阳极单电池,最大功率密度为 287 mW·cm⁻² (氢气) 和 210 mW·cm⁻² (乙醇),而 LSCM-YSZ2010 阳极单电池,最大功率密度分别达到 656 mW·cm⁻² (氢气) 和 492 mW·cm⁻² (乙醇). 然而, 随着 Cu 含量的增加,750 °C 时 LSCM-YSZ3010 阳极单电池最大功率却只有 327 mW·cm⁻² (氢气) 和 294 mW·cm⁻² (乙醇). 800 °C 时,其最大功率密度为 419 mW·cm⁻² (氢气) 和 371 mW·cm⁻² (乙醇). 随阳极催化层中 Cu 含量增加,单电池性能先增加后反而下降. 电化学交流阻抗谱图 (图 3、4) 也证实了随着阳极催化层 Cu 含量增加,其电池的欧姆电阻和极化电阻也出现先减小后增加的趋势. 同一单电池,乙醇燃料极化电阻比氢气极化电阻稍有增加. Cu 颗粒不仅构成了阳极导电网络,尤其连通了各个反应活性点位. 因此, CeO₂ 含量达到一定值,其量再增加对提高阳极性能并无太大裨益,此时掺入更多 Cu,不仅能提高阳极的电导率,还能连接更多的反应活性点位,增加阳极三相界面长度^[33-34]. 乙醇的分子量比氢气的大得多,二者的扩散速率也相差甚多,另一种可能原因就是燃料自身的差异,作为还原剂,乙醇的活性显然比氢气的差得多,这就导致更高的极化电阻

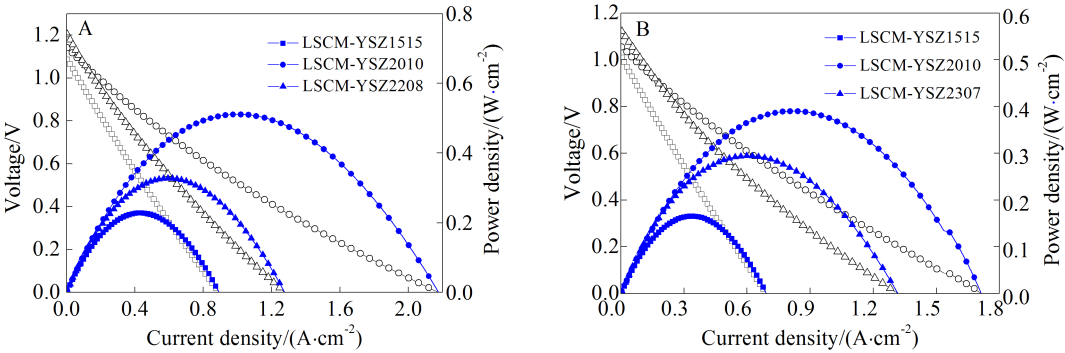


图 1 LSCM-YSZ1515、LSCM-YSZ2010 和 LSCM-YSZ3010 阳极单电池氢气(A)和乙醇蒸汽(B)燃料(750 °C)的 I - V 和 I - P 曲线

Fig. 1 Voltage and power density vs. current density curves for an SOFC with LSCM-YSZ1515, LSCM-YSZ2010 and LSCM-YSZ3010 anodes while running on hydrogen (A) and ethanol steam (B) at 750 °C

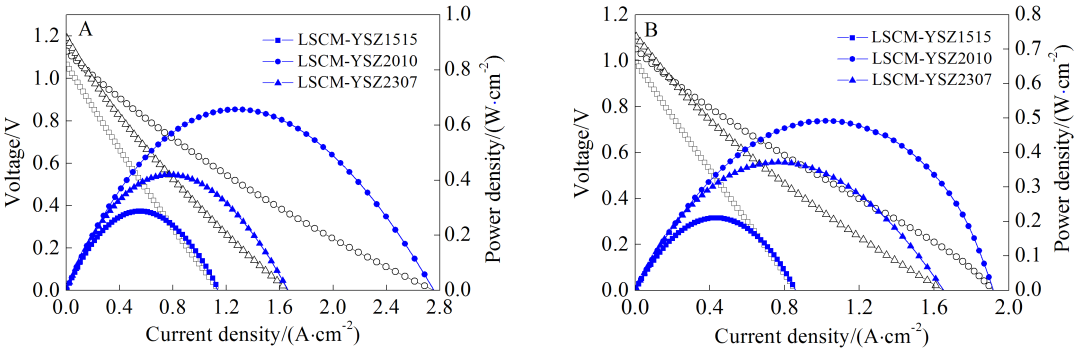


图 2 LSCM-YSZ1515、LSCM-YSZ2010 和 LSCM-YSZ3010 阳极单电池氢气(A)和乙醇蒸汽(B)燃料(800 °C)的 I - V 和 I - P 曲线

Fig. 2 Voltage and power density vs. current density curves for an SOFC with LSCM-YSZ1515, LSCM-YSZ2010 and LSCM-YSZ3010 anodes while running on hydrogen (A) and ethanol steam (B) at 800 °C

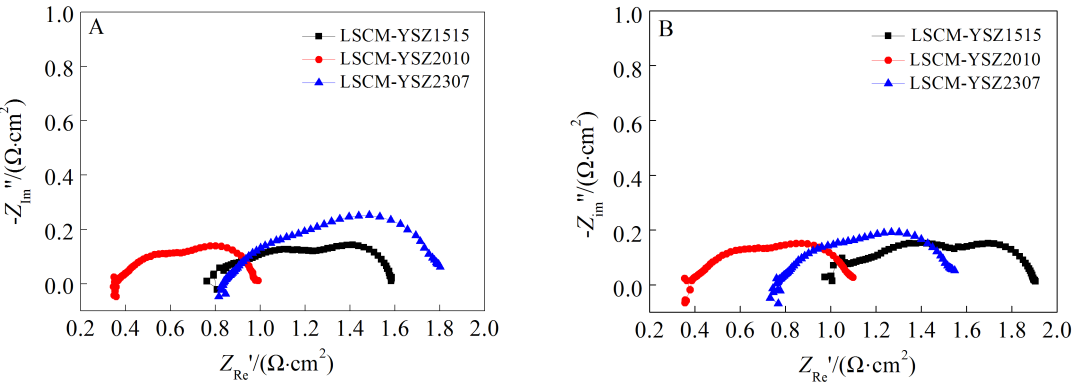


图 3 LSCM-YSZ1515、LSCM-YSZ2010 和 LSCM-YSZ3010 阳极单电池氢气(A)和乙醇蒸汽(B)燃料(750 °C)的阻抗谱图

Fig. 3 Electrochemical impedance spectra for an SOFC with LSCM-YSZ1515, LSCM-YSZ2010 and LSCM-YSZ3010 anodes while running on hydrogen (A) and ethanol steam (B) at 750 °C

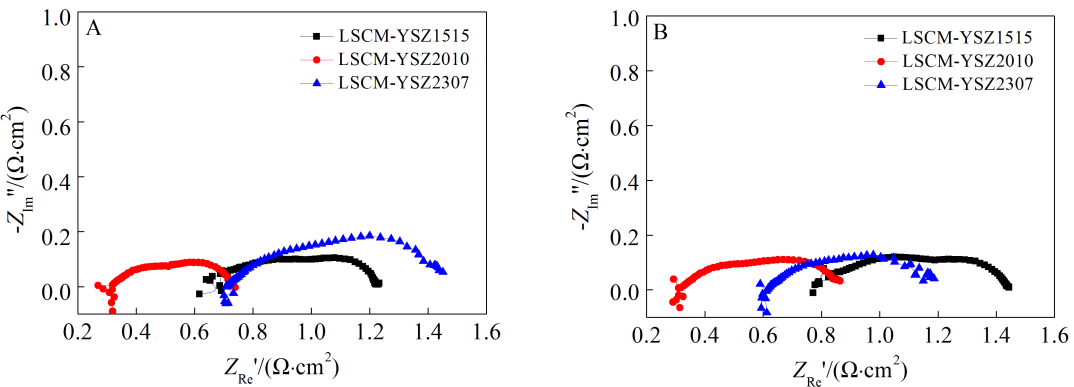


图 4 LSCM-YSZ1515、LSCM-YSZ2010 和 LSCM-YSZ3010 阳极单电池氢气(A)和乙醇蒸汽(B)燃料(800 °C)阻抗谱图

Fig. 4 Electrochemical impedance spectra for an SOFC with LSCM-YSZ1515, LSCM-YSZ2010 and LSCM-YSZ3010 anodes while running on hydrogen (A) and ethanol steam (B) at 800 °C

以及较慢的电化学氧化. 这些因素决定了乙醇燃料极化面电阻远大于其在氢气的数值, 其电化学

性能自然相对较差. LSCM-YSZ3010 阳极单电池欧姆电阻随 Cu 含量的增加反而增加, 可能是由于

高温操作时 Cu 颗粒分散不均匀, 以及 Cu 颗粒的烧结和质量转移导致阳极导电通路的减少, 从而降低了阳极的电导率. 同时, 过多的掺入 Cu 也降低了阳极的催化性能, 导致电池性能降低.

图 5 为三组单电池乙醇为燃料(750 °C, 0.6 V) $w-t$ 曲线. 从该图可发现, 三组电池在该条件下随时间变化功率基本不变, 且以 LSCM-YSZ2010 为阳极的单电池功率密度随时间变化有微小的波动, 可能是由于操作控制气流时导致乙醇蒸汽供应的不稳定而引起的, 运行 218 h, 其功率密度几乎维持不变($200\text{ mW}\cdot\text{cm}^{-2}$), 说明该阳极单电池可较长时间稳定工作.

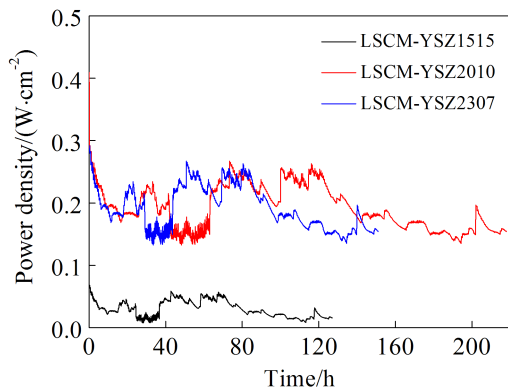


图 5 以 LSCM-YSZ1515、LSCM-YSZ2010 和 LSCM-YSZ3010 阳极单电池乙醇燃料(750 °C, 0.6 V) $w-t$ 曲线

Fig. 5 Power density vs. time curves of an SOFC with the LSCM-YSZ1515、LSCM-YSZ2010 and LSCM-YSZ3010 anodes using ethanol steam as fuel and oxygen as oxidant while discharging under 0.6 V at 750 °C during the aging process

3 扫描电镜分析

图 6 示出 Cu-LSCM-CeO₂/LSCM-YSZ/Ni-ScSZ/ScSZ/PCM 断面的 SEM 照片. 从照片可以看出, Cu-LSCM-CeO₂ 催化层、LSCM-YSZ 支撑层、Ni-ScSZ 活性层、ScSZ 电解质层和 PCM 阴极层. 其电化学反应发生于三相界面, 因而阳极的微观对电池的性能有很大的影响. 长时间运行的阳极支撑层与阳极催化层及其界面的断面 SEM 显微结构照片图 7 所示: LSCM-YSZ2010 阳极单电池两层间结合良好, 没有很明显的分层, 颗粒大小均匀, 仍有良好的多孔结构. 扫描电子显微镜

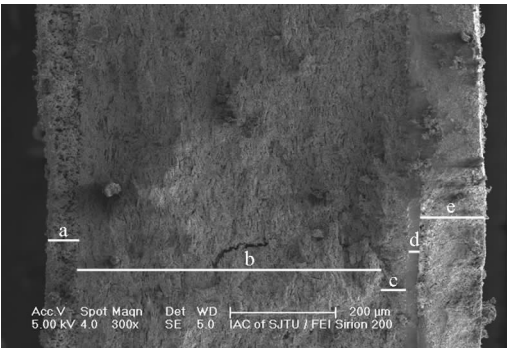


图 6 单电池 Cu-LSCM-CeO₂/LSCM-YSZ/Ni-ScSZ/ScSZ/PCM 断面的 SEM 照片

a. Cu-LSCM-CeO₂ 催化层; b. LSCM-YSZ 支撑层; c. Ni-ScSZ 活性层; d. ScSZ 电解质层; e. PCM 阴极层

Fig. 6 SEM micrograph of a fractured single cell showing five layers

a. porous Cu-LSCM-CeO₂ catalyst layer; b. porous LSCM-YSZ support layer; c. porous Ni-ScSZ active layer; d. dense ScSZ electrolyte layer; e. porous PCM cathode layer

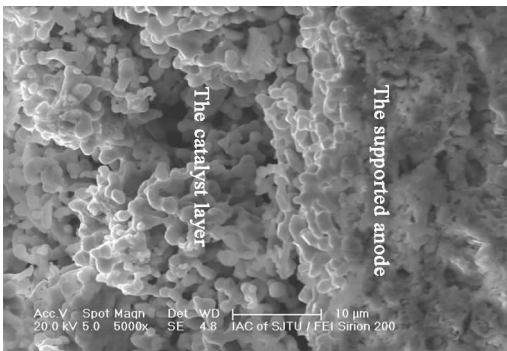


图 7 LSCM-YSZ2010 为阳极的单电池阳极 SEM 照片

Fig. 7 SEM cross-sectional micrograph of the LSCM-YSZ2010 anode

和 X-射线能量散射分析谱 (EDAX) 显示 LSCM-YSZ2010 阳极仅有少量碳沉积(图 8), 有较好的抗碳沉积性能.

4 结 论

三层流延法 LSCM-YSZ 支撑层 /Ni-ScSZ 活性层 /ScSZ 电解质层复合膜, 在烧结的 LSCM-YSZ 支撑层上丝网印刷一层 Cu-LSCM-CeO₂ 催化层, 并制得 Cu/LSCM/CeO₂ 不同配比功能梯度阳极的单电池. LSCM-YSZ2010 阳极单电池性氢气和乙醇蒸汽为燃料时(750 °C)

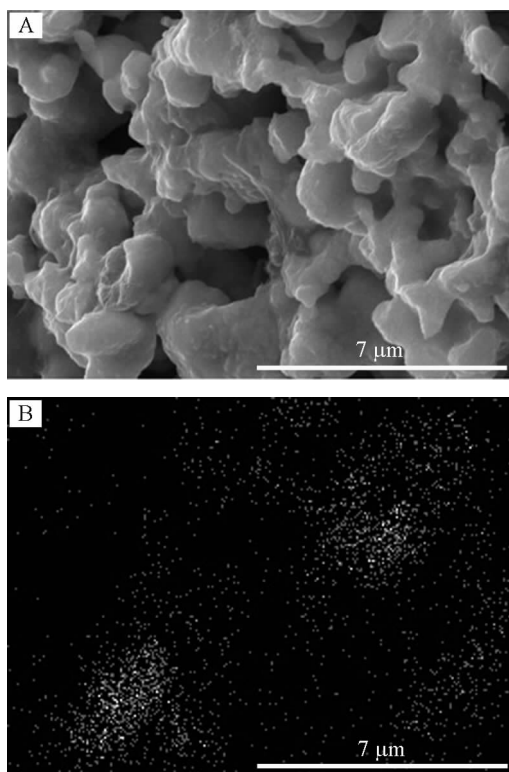


图 8 LSCM-YSZ2010 为阳极单电池以乙醇为燃料(750℃)运行 218 h 的电子探针显微照片:A. 阳极自由面的 SEM 照片;B. 阳极自由面的碳沉积照片

Fig. 8 Electron probe microscopic analysis (EPMA) of the LSCM-YSZ2010 anode operated in ethanol fuel at 750 °C under an open circuit condition for 218 h: A. SEM image of the anode free surface; B. C mapping of the anode free surface

最大功率密度为 511 和 390 $\text{mW} \cdot \text{cm}^{-2}$ 。218 h 长时间运行后,其性能仅略有下降,有较好的抗碳沉积性。

参考文献 (References):

- [1] Lawlor V, Griesser S, Buchinger G, et al. Review of the micro-tubular solid oxide fuel cell: Part I. Stack design issues and research activities[J]. Journal of power sources, 2009, 193(2): 387-399.
- [2] Suzuki T, Yamaguchi T, Fujishiro Y, et al. Improvement of SOFC performance using a microtubular, anode-supported SOFC[J]. Journal of the Electrochemical Society, 2006, 153(5): A925-A928.
- [3] Lee T J, Kendall K. Characterisation of electrical performance of anode supported micro-tubular solid oxide fuel cell with methane fuel[J]. Journal of Power Sources, 2008, 181(2): 195-198.
- [4] Steele B C H. Fuel-cell technology: Running on natural gas[J]. Nature, 1999, 400(6745): 619-621.
- [5] Zhan Z, Barnett S A. An octane-fueled solid oxide fuel cell [J]. Science, 2005, 308(5723): 844-847.
- [6] Gunji A, Wen C, Otomo J, et al. Carbon deposition behaviour on Ni-ScSZ anodes for internal re forming solid oxide fuel cells[J]. Journal of power sources, 2004, 131(1): 285-288.
- [7] Gorte R J, Vohs J M. Novel SOFC anodes for the direct electrochemical oxidation of hydrocarbons[J]. Journal of catalysis, 2003, 216(1): 477-486.
- [8] Park S, Craciun R, Vohs J M, et al. Direct oxidation of hydrocarbons in a solid oxide fuel cell: I. Methane oxidation [J]. Journal of the Electrochemical Society, 1999, 146(10): 3603-3605.
- [9] McIntosh S, Vohs J M, Gorte R J. An examination of lanthanide additives on the performance of Cu-YSZ cermet anodes[J]. Electrochimica acta, 2002, 47(22): 3815-3821.
- [10] McIntosh S, Gorte R J. Direct hydrocarbon solid oxide fuel cells[J]. Chemical Reviews, 2004, 104(10): 4845-4866.
- [11] Brett D J L, Atkinson A, Cumming D, et al. Methanol as a direct fuel in intermediate temperature solid oxide fuel cells with copper based anodes[J]. Chemical Engineering Science, 2005, 60(21): 5649-5662.
- [12] Sun C, Stimming U. Recent anode advances in solid oxide fuel cells[J]. Journal of Power Sources, 2007, 171(2): 247-260.
- [13] Murray E P, Tsai T, Barnett S A. A direct-methane fuel cell with a ceria-based anode[J]. Nature, 1999, 400(6745): 649-651.
- [14] Qi X, Flytzani-Stephanopoulos M. Activity and stability of Cu-CeO₂ catalysts in high-temperature water-gas shift for fuel-cell applications [J]. Industrial & engineering chemistry research, 2004, 43(12): 3055-3062.
- [15] Bi Z H, Zhu J H. A Cu-CeO₂-LDC composite anode for LSGM electrolyte-supported solid oxide fuel cells [J]. Electrochemical and Solid-State Letters, 2009, 12 (7): B107-B111.
- [16] Qiao J, Zhang N, Wang Z, et al. Performance of mix impregnated CeO₂ Ni/YSZ anodes for direct oxidation of methane in solid oxide fuel cells[J]. Fuel Cells, 2009, 9 (5): 729-739.
- [17] Ye X F, Zhou J, Wang S R, et al. Research of carbon deposition formation and judgment in Cu-CeO₂-ScSZ anodes for direct ethanol solid oxide fuel cells[J]. International Journal of Hydrogen Energy, 2012, 37(1): 505-510.
- [18] Tao S, Irvine J T S. A redox-stable efficient anode for solid-oxide fuel cells[J]. Nature Materials, 2003, 2(5): 320-323.
- [19] Tao S, Irvine J T S. Synthesis and characterization of

- (La_{0.75}Sr_{0.25})Cr_{0.5}Mn_{0.5}O_{3-δ}, a redox-stable, efficient perovskite anode for SOFCs[J]. *Journal of The Electrochemical Society*, 2004, 151(2): A252-A259.
- [20] Périllat-Merceroz C, Gauthier G, Roussel P, et al. Synthesis and study of a Ce-doped La/Sr titanate for solid oxide fuel cell anode operating directly on methane[J]. *Chemistry of Materials*, 2011, 23(6): 1539-1550.
- [21] Kim J H, Miller D, Schlegel H, et al. Investigation of microstructural and electrochemical properties of impregnated (La, Sr)(Ti, Mn) O_{3-δ} as a potential anode material in high-temperature solid oxide fuel cells[J]. *Chemistry of Materials*, 2011, 23(17): 3841-3847.
- [22] Monteiro N K, Noronha F B, Da Costa L O O, et al. A direct ethanol anode for solid oxide fuel cell based on a chromite-manganite with catalytic ruthenium nanoparticles[J]. *International Journal of Hydrogen Energy*, 2012, 37(12): 9816-9829.
- [23] Zhan Z, Barnett S A. An octane-fueled solid oxide fuel cell[J]. *Science*, 2005, 308(5723): 844-847.
- [24] Zhan Z, Lin Y, Pillai M, et al. High-rate electrochemical partial oxidation of methane in solid oxide fuel cells[J]. *Journal of power sources*, 2006, 161(1): 460-465.
- [25] Jiang S P, Chan S H. Review of anode materials development in solid oxide fuel cells[J]. *Journal of Materials Science*, 2004, 39(14): 4405-4439.
- [26] Wang W, Ran R, Shao Z. Combustion-synthesized Ru-Al₂O₃ composites as anode catalyst layer of a solid oxide fuel cell operating on methane[J]. *International Journal of Hydrogen Energy*, 2011, 36(1): 755-764.
- [27] Hornés A, Bera P, Fernández-García M, et al. Catalytic and redox properties of bimetallic Cu-Ni systems combined with CeO₂ or Gd-doped CeO₂ for methane oxidation and decomposition[J]. *Applied Catalysis B: Environmental*, 2012, 111: 96-105.
- [28] Yun J W, Yoon S P, Kim H S, et al. Effect of Sm_{0.2}Ce_{0.8}O_{1.9} on the carbon coking in Ni-based anodes for solid oxide fuel cells running on methane fuel[J]. *International Journal of Hydrogen Energy*, 2012, 37(5): 4356-4366.
- [29] Zhu H, Wang W, Ran R, et al. A new nickel-ceria composite for direct-methane solid oxide fuel cells [J]. *International Journal of Hydrogen Energy*, 2013, 38(9): 3741-3749.
- [30] Jin C, Yang C, Zheng H, et al. Intermediate temperature solid oxide fuel cells with Cu_{1.3}Mn_{1.7}O₄ internal reforming layer[J]. *Journal of Power Sources*, 2012, 201: 66-71.
- [31] Bo Huang, S.R. Wang, R.Z. Liu, et al. Performance of La_{0.75}Sr_{0.25}Cr_{0.5}Mn_{0.5}O_{3-δ} perovskite-structure anode material at lanthanum gallate electrolyte for IT-SOFC running on ethanol fuel[J]. *Journal of Power Sources*, 2007, 167(1): 39-46.
- [32] Ye X F, Wang S R, Wang Z R, et al. Use of a catalyst layer for anode-supported SOFCs running on ethanol fuel [J]. *Journal of Power Sources*, 2008, 177(2): 419-425.
- [33] Ioselevich A, Kornyshev A A, Lehnert W. Statistical geometry of reaction space in porous cermet anodes based on ion-conducting electrolytes: Patterns of degradation [J]. *Solid State Ionics*, 1999, 124(3): 221-237.
- [34] Ioselevich A, Kornyshev A A, Lehnert W. Degradation of solid oxide fuel cell anodes due to sintering of metal particles correlated percolation model [J]. *Journal of the Electrochemical Society*, 1997, 144(9): 3010-3019.

Fabrication and Characterization of the Ni-ScSZ Composite Anodes with a Cu-LSCM-CeO₂ Catalyst Layer in the Thin Film SOFC

LV Yao, HUANG Bo*, GU Xi-zhi, HOU Chun-yi, HU Yi-xing, WANG Xiao-ying, ZHU Xin-jian
(*Institute of Fuel Cell, School of Mechanical Engineering, Shanghai Jiaotong University, Shanghai 200240, China*)

Abstract: Solid oxide fuel cell (SOFC) directly operating on hydrocarbon without external reforming has the potential of greatly speeding up the application of SOFCs for transportation. In this paper, a three-layer structure anode was fabricated by tape casting and screen printing method. The addition of Cu-LSCM-CeO₂ to the supported anode surface presented better performance running on H₂ and ethanol. The maximum power densities were 511 and 390 mW·cm⁻², respectively running on H₂ and ethanol at 750 °C. No significant degradation was observed on the anode. Consequently, the Cu-LSCM-CeO₂ catalyst layer on the surface of the LSCM-YSZ support layer makes it possible to have good stability for long-term operation in ethanol fuel due to free carbon deposition.

Key words: solid oxide fuel cell; catalyst layer; carbon deposit; impedance spectra; electrochemical performance